



## Effect of annealing temperature on magnetic property of $\text{Si}_{1-x}\text{Cr}_x$ thin films

Wenyong Zhang, Liping Guo\*, Guoliang Peng, Tiecheng Li, Shixuan Feng, Zhongpo Zhou, Ting Peng, Zuci Quan

Key Laboratory of Artificial Micro- and Nano-structures of Ministry of Education and School of Physics and Technology, Wuhan University, Wuhan 430072, China

### ARTICLE INFO

Available online 2 February 2011

#### Keywords:

Magnetron sputtering  
Diluted magnetic semiconductors  
Rapid thermal annealing  
X-ray diffraction  
Raman spectra

### ABSTRACT

Polycrystalline  $\text{Si}_{1-x}\text{Cr}_x$  thin films have been prepared by magnetron sputtering followed by rapid thermal annealing (RTA) for crystallization. RTA was performed at 800 °C for 5 min, 1200 °C for 30 s and 1200 °C for 2 min, in a  $\text{N}_2$  flow. The magnetic hysteresis loops were observed at room temperature in all the samples except for RTA at 800 °C for 5 min, and the annealing caused the decrease of saturation magnetization relative to the as-grown film. X-ray diffraction spectra and Raman spectra showed that the annealing process lead the deposited amorphous film to be crystallized and  $\text{CrSi}_2$  phase formed. The magnetism of the films was determined by the competition between crystallinity and precipitation of diamagnetic  $\text{CrSi}_2$  phase.

© 2011 Elsevier B.V. All rights reserved.

### 1. Introduction

As one of the most promising materials for spintronic devices, diluted magnetic semiconductors (DMSs) have attracted much attention in recent years [1,2]. Si-based DMSs, prepared by doping transition-metal atoms such as Mn, Cr and Co into silicon substrate, were especially interesting owing to their compatibility with the mature technologies of silicon industry [3–5].

Recently, extensive studies on  $\text{Si}_{1-x}\text{Mn}_x$  DMSs were carried out [6–9]. Bolduc et al. prepared the  $\text{Si}_{1-x}\text{Mn}_x$  films by Mn ion implantation and found room temperature ferromagnetism in the films [10–12]. Zhou et al. reported that  $\text{MnSi}_{1.7}$  nanoparticles existed in  $\text{Si}_{1-x}\text{Mn}_x$  DMSs prepared by ion implantation, whose size increased from 5 nm to 20 nm upon rapid thermal annealing [13]. Zhang et al. investigated crystalline  $\text{Mn}_{0.05}\text{Si}_{0.95}$  films prepared by post-thermal treatment of the as-deposited amorphous film and found ferromagnetism with Curie temperature over 400 K [14]. However, the investigations on magnetic property of  $\text{Si}_{1-x}\text{Cr}_x$  DMSs are relatively rare [15]. Gao et al. [16] investigated the magnetism of  $\text{Si}_{1-x}\text{Cr}_x$  DMSs prepared by ion implantation and found robust room temperature ferromagnetism. Yao et al. [17,18] prepared amorphous  $\text{Si}_{1-x}\text{Cr}_x$  films by magnetron sputtering on glass substrate to study the effect of hydrogenation and demonstrated that hydrogenation could enhance saturation magnetization by about 100%. In the present paper, we prepared amorphous  $\text{Si}_{1-x}\text{Cr}_x$  films by magnetron sputtering on single crystal silicon substrate, and different processes of annealing were performed to investigate the effect of annealing on the properties of magnetism and structure.

### 2. Experimental details

Cr-doped amorphous silicon films were deposited on p-type Si (100) single crystal wafer by radio frequency (RF) magnetron sputtering at room temperature. Single crystal Si was used as the target and it was partially covered with highly purified (99.99%) Cr chips for incorporation of Cr into the films. With a base pressure of  $7.8 \times 10^{-4}$  Pa, the operation pressure and power were 3.2 Pa and 100 W, respectively. After deposition, the samples were annealed at

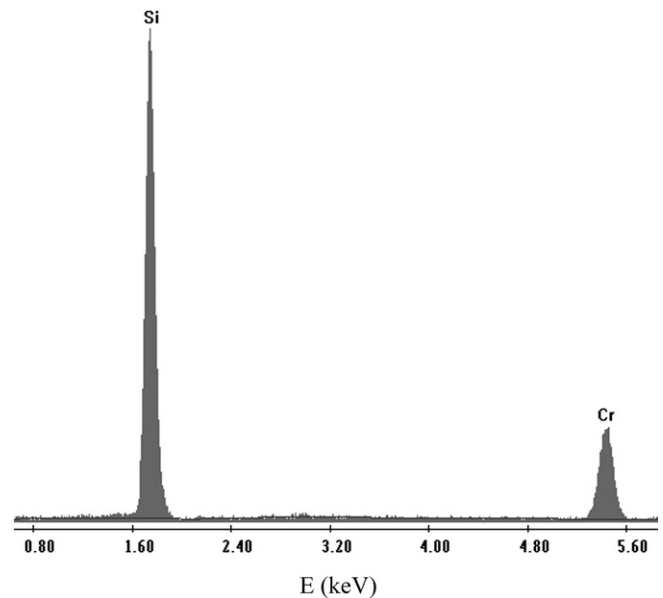


Fig. 1. EDS map of sample A (as-grown  $\text{Si}_{1-x}\text{Cr}_x$  film).

\* Corresponding author at: School of Physics and Technology, Wuhan University, Wuhan 430072, China. Tel.: +86 27 6875 3587; fax: +86 27 6875 2569.

E-mail address: [guolp@whu.edu.cn](mailto:guolp@whu.edu.cn) (L. Guo).

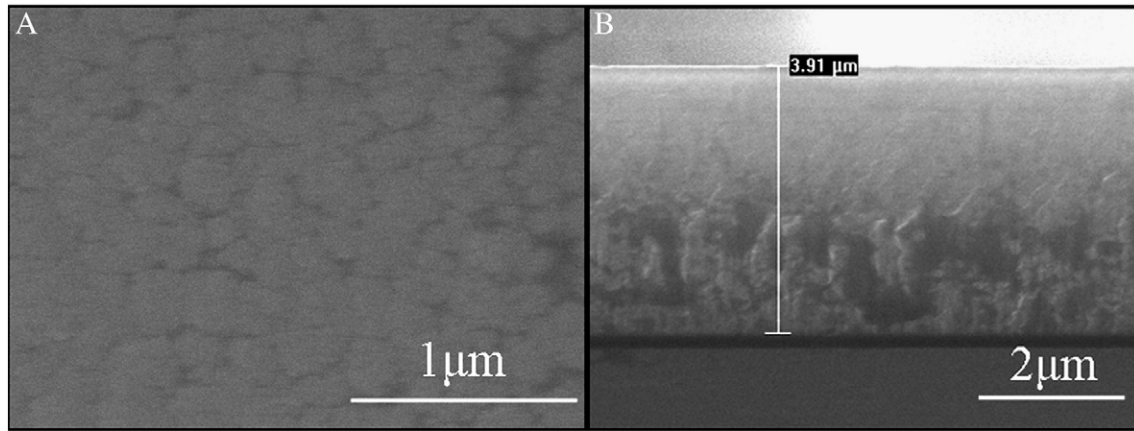


Fig. 2. SEM images of sample A (as-grown  $\text{Si}_{1-x}\text{Cr}_x$  film). (A) Surface image, (B) cross-section image.

800 °C for 5 min, 1200 °C for 30 s and 1200 °C for 2 min in flowing  $\text{N}_2$  gas. The three films were marked as sample B, sample C and sample D, while the as-grown film was sample A. The structure of the films was analyzed through X-ray diffraction (XRD, Bruker-axs D8 Advanced) with  $\text{Cu K}\alpha$  radiation. The Cr atom concentration of the films was detected with an EDAX Genesis 7000 energy dispersive spectroscopy (EDS) system. The morphology of the films was observed by scanning electron microscopy (SEM, FEI SironMP) and atomic force microscope (AFM, Shimadzu SPM-9500J3). Micro-Raman scattering spectra were measured on a Laser Confocal Raman Microspectroscopy with the 632.6 nm line of a He-Ne laser as excitation source (LabRAM HR 800 UV, France). Alternating gradient magnetometer (AGM, PMC 2900-04C) was employed to investigate the magnetic property at room temperature.

### 3. Results and discussion

After deposition, the as-grown film was examined by EDS to detect the concentration of Cr. As shown in Fig. 1, Si and Cr peaks were visible and the small O peak that appeared might be due to surface oxygen pollution. After ZAF correction, the Cr atom concentration was 12.17%, which was under the solubility limit of Cr in Si [17]. From SEM images of sample A (Fig. 2), the thickness of the film was estimated to be 3.91  $\mu\text{m}$  and the surface was smooth. The SEM result indicated that the as-grown film was amorphous.

Fig. 3 showed the surface morphology of the films with  $5 \mu\text{m} \times 5 \mu\text{m}$  scanning area. The root mean square roughness (RMS) of sample A was 7.36 nm, and sample B was rougher than sample A, with a RMS of 9.50 nm. The surface morphology of samples C and D was much

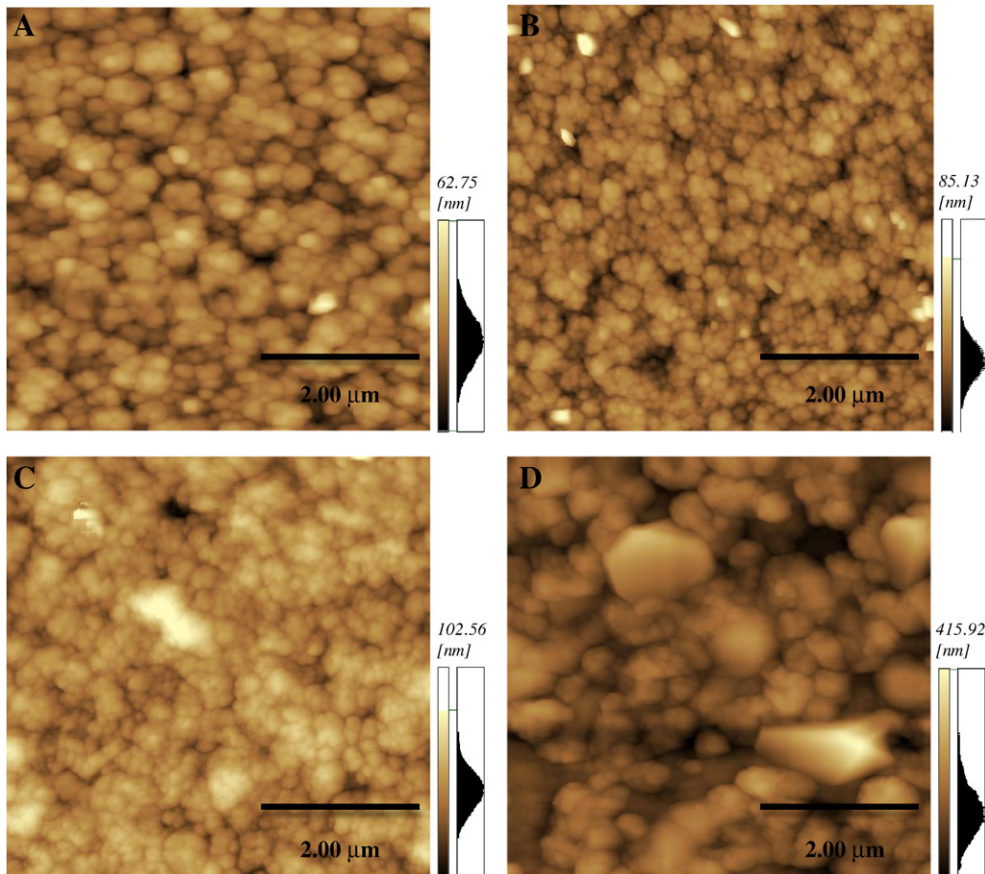


Fig. 3. AFM morphologies of samples: (A) as-grown, (B) 800 °C, 5 min, (C) 1200 °C, 30 s, (D) 1200 °C, 2 min.

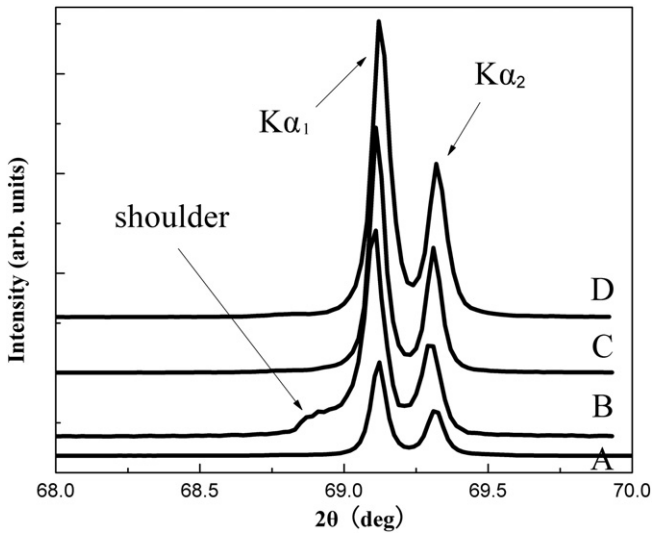


Fig. 4. Si (400) X-ray diffraction peak of the samples. (A) As-grown, (B) 800 °C, 5 min, (C) 1200 °C, 30 s, (D) 1200 °C, 2 min.

different from samples A and B: big island-like humps were clearly recognized. When the annealing time was increased from 30 s to 2 min at 1200 °C, the RMS was changed from 12.86 nm to 52.03 nm, and the humps became bigger and sharpened edges appeared, manifesting the existence of crystalline grain on the surface. The result of AFM suggested that the films had the tendency to be crystallized after 1200 °C temperature annealing process.

Fig. 4 showed the Si (400) diffraction peaks of the samples. It was interesting that a shoulder peak appeared for sample B, while this peak was not observed for the other three samples. The shoulder peak may be attributed to the presence of substitutional  $\text{Cr}^{+}$  ions in the Si lattice under 800 °C annealing, resembling to the situation of  $\text{Si}_{1-x}\text{Mn}_x$  films [19,20]. For samples C and D, both annealed at 1200 °C, the absence of a shoulder peak may indicate that  $\text{Cr}^{+}$  ions escaped from the silicon lattice after higher temperature annealing.

XRD patterns other than Si (400) diffraction peaks were shown in Fig. 5. All the diffraction peaks were attributed to  $\text{CrSi}_2$  except for the Si (200) peak. The broadening of Si (200) peak indicated that the films were not completely crystallized and the crystal size was very small. A weak  $\text{CrSi}_2$  (200) peak appeared for sample B, and more  $\text{CrSi}_2$  peaks can be found for samples C and D when RTA temperature rose to

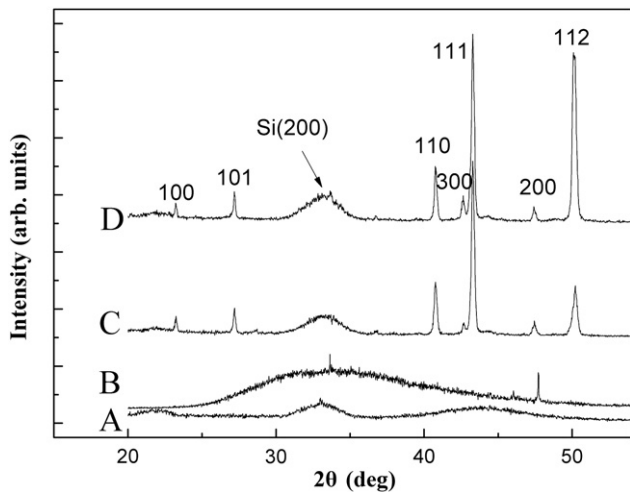


Fig. 5. XRD patterns of the samples. (A) As-grown, (B) 800 °C, 5 min, (C) 1200 °C, 30 s, (D) 1200 °C, 2 min.

1200 °C. These results showed that the crystal  $\text{CrSi}_2$  formed during crystallization of the films, and  $\text{CrSi}_2$  crystal was growing during the annealing process.

Raman spectra were shown in Fig. 6. For sample A, amorphous silicon peak around  $480\text{ cm}^{-1}$  [21] can be found from the graph. This amorphous peak disappeared after annealing. The sharpest and strongest peak at  $296\text{ cm}^{-1}$  could be assigned to  $E_1$  (TO) mode of  $\text{CrSi}_2$  [22,23]. This peak became sharper and higher with the increasing of RTA time, indicating that the  $\text{CrSi}_2$  crystal grew larger. The Raman shift of 227, 250, 349 and  $391\text{ cm}^{-1}$  could be also attributed to  $\text{CrSi}_2$  [24–26]. The Raman shifts around  $517\text{ cm}^{-1}$  of sample C and  $523\text{ cm}^{-1}$  of sample D were related to crystalline silicon [4], and the wavenumber shift indicated the improvement of crystallinity of the samples. For sample D, the band centered at  $550\text{ cm}^{-1}$  was attributed to the  $A_{1g}$  symmetry of  $\text{Cr}_2\text{O}_3$  and the band centered at  $608\text{ cm}^{-1}$  was attributed to the  $E_g$  symmetry of  $\text{Cr}_2\text{O}_3$  [27]. Our Raman results indicated that the main component in the near-surface region of the annealed samples was  $\text{CrSi}_2$ , and  $\text{Cr}_2\text{O}_3$  appeared when annealed at 1200 °C for 2 min. The annealing process led the deposited amorphous film to be crystallized and  $\text{CrSi}_2$  phase formed.

The magnetization versus magnetic field curves (M–H curves) at room temperature was shown in Fig. 7. The diamagnetic silicon substrate was subtracted and ferromagnetism could be discovered in sample A with the saturation magnetization ( $M_s$ ) of  $1.8 \times 10^{-2}\text{ A m}^2/\text{kg}$ . Sample B exhibited a very weak S-shape loop, indicating the absence of ferromagnetism when annealed at 800 °C for 5 min. When annealed at 1200 °C, the magnetism was also quite weak and each loop showed an S-shape with the saturation magnetic moment of  $9.2 \times 10^{-3}\text{ A m}^2/\text{kg}$  and  $8.4 \times 10^{-3}\text{ A m}^2/\text{kg}$  for samples C and D, respectively. The result of M–H hysteresis loops showed that the effect of annealing on magnetism

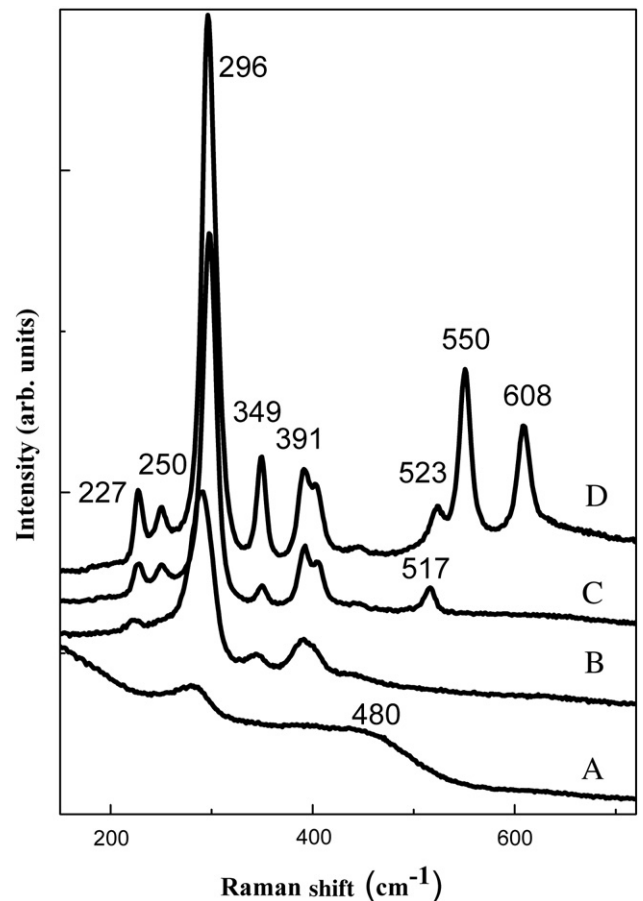


Fig. 6. Raman spectra of the samples. (A) As-grown, (B) 800 °C, 5 min, (C) 1200 °C, 30 s, (D) 1200 °C, 2 min.

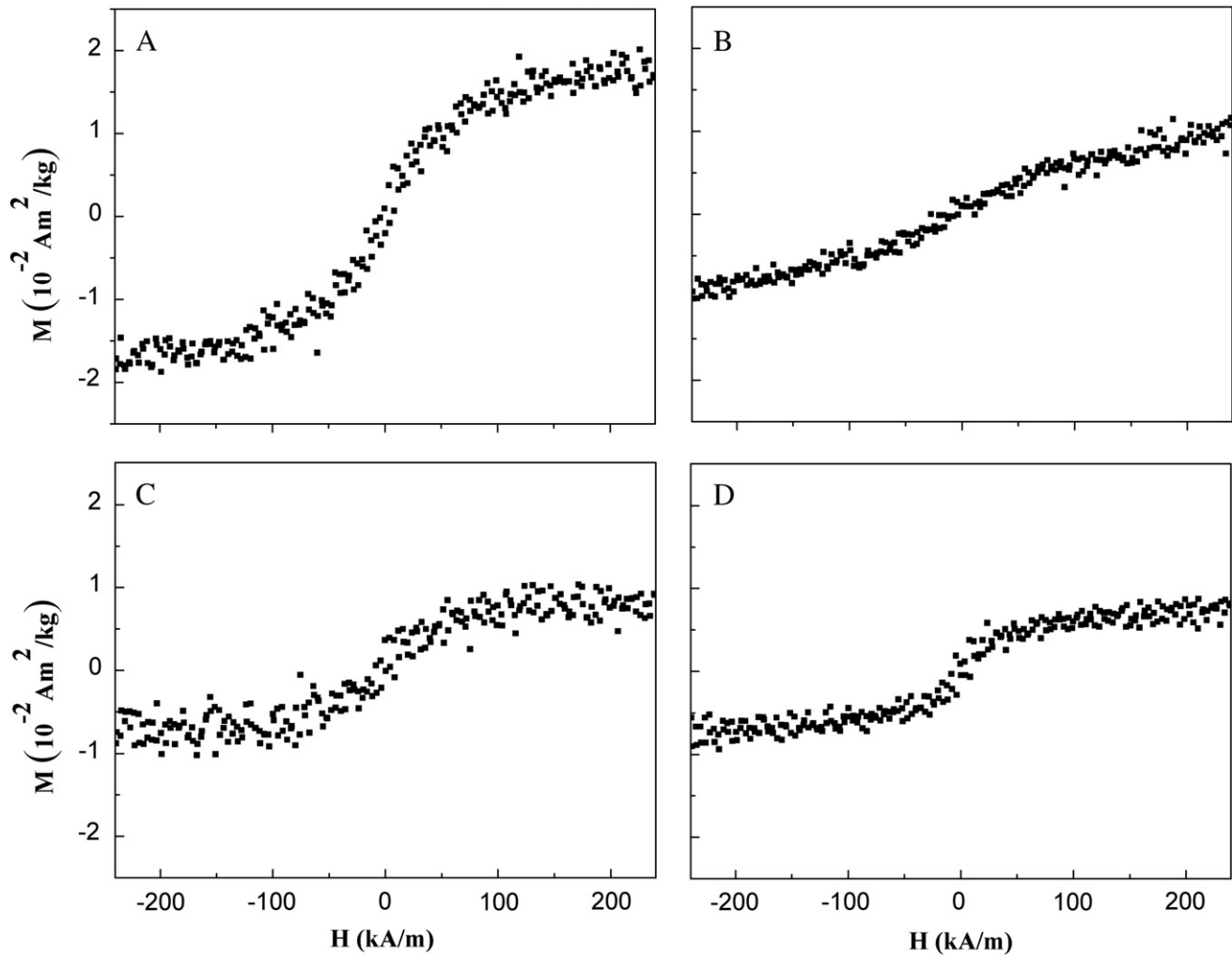


Fig. 7. M–H curves for the samples at room temperature. (A) As-grown, (B) 800 °C, 5 min, (C) 1200 °C, 30 s, (D) 1200 °C, 2 min.

was complex, not just only leading to the absence of ferromagnetism as another paper reported [16].

Unlike the effect of annealing on  $\text{Si}_{1-x}\text{Mn}_x$  films where  $M_s$  increased [19,28], the  $M_s$  decreased after annealing for  $\text{Si}_{1-x}\text{Cr}_x$  films. Based on the results of AFM, XRD and Raman spectra, the annealing process led the crystallization of silicon and the formation of  $\text{CrSi}_2$ . Note that Cr and  $\text{Cr}_2\text{O}_3$  were anti-ferromagnetic [29] and pure silicon and  $\text{CrSi}_2$  were diamagnetic [30], these crystallized phases have no contribution to the ferromagnetism. In the situation of sample B, although the presence of substitutional  $\text{Cr}^+$  ions in Si lattice was found, ferromagnetism was absent, suggesting that the only existence of substitutional  $\text{Cr}^+$  might have no contribution to ferromagnetism [19].

According to the percolation theory of magnetic polaron [17,31], the exchange interaction of localized holes with magnetic impurities leads to the formation of bound magnetic polarons and the interaction between the polarons might be ferromagnetic at large enough concentration of impurities [31]. After annealing, the interaction between magnetic polarons decreased with the appearance of diamagnetic  $\text{CrSi}_2$ , consequently the saturation magnetic moment and led to the absence of ferromagnetism for sample B. However, annealing would also lead the deposited amorphous film to be crystallized, and this tendency would improve carrier density and enhance the carrier-mediated ferromagnetic interaction [18]. This carrier-mediated ferromagnetic interaction might slow down the decrease of  $M_s$  and results in magnetic hysteresis loops that appeared again after annealing at 1200 °C. It should be noticed that the foregoing discussion about ferromagnetism was just speculative, and

more investigations are needed to be carried out to elucidate the mechanism of ferromagnetism.

#### 4. Conclusion

In summary,  $\text{Si}_{1-x}\text{Cr}_x$  films were prepared by magnetron sputtering and performed by different RTA processes. The microstructure was analyzed by SEM, AFM, XRD and Raman spectra, and the results showed that the as-grown amorphous  $\text{Si}_{1-x}\text{Cr}_x$  films tended to be crystallized and  $\text{CrSi}_2$  precipitated after annealing. The as-grown film exhibited strongest room temperature ferromagnetism, and the annealing has a complex effect on the magnetic property of the films. The magnetism of the films was ascribed to the competition between crystallinity and precipitation of diamagnetic  $\text{CrSi}_2$  phase.

#### Acknowledgements

The present work was supported by the National Natural Science Foundation of China (Grant No. 10775108), PhD Independent Research Fund of Wuhan University (Grant No. 20102020201000034) and National Science Fund for Talent Training in Basic Science (Grant No. J0830310).

#### References

- [1] T. Dietl, H. Ohno, F. Matsukura, J. Cibert, D. Ferrand, *Science* 287 (2000) 1019.
- [2] S.J. Sun, H.H. Lin, *Phys. Lett. A* 327 (2004) 73.

- [3] L.F. Liu, N.F. Chen, S.L. Song, Z.G. Yin, F. Yang, C.L. Chai, S.Y. Yang, Z.K. Liu, J. Cryst. Growth 273 (2005) 458.
- [4] I.T. Yoon, C.J. Park, S.W. Lee, T.W. Kang, D.J. Fu, X.J. Fan, Solid State Commun. 140 (2006) 185.
- [5] A. Wolska, K. Lawniczak-Jablonska, M. Klepka, M. Walczak, A. Misiuk, Phys. Rev. B 75 (2007) 113201.
- [6] I.T. Yoon, C.J. Park, T.W. Kang, J. Magn. Mater. 311 (2007) 693.
- [7] O. Picht, W. Wesch, J. Biskupek, U. Kaiser, M.A. Oliveira, A. Neves, N.A. Sobolev, Nucl. Instrum. Methods B 257 (2007) 90.
- [8] V. Ko, K.L. Teo, T. Liew, T.C. Chong, M. MacKenzie, I. MacLaren, J.N. Chapman, J. Appl. Phys. 104 (2008) 033912.
- [9] L. Zeng, E. Helgren, M. Rahimi, F. Hellman, R. Islam, B.J. Wilkens, R.J. Culbertson, D.J. Smith, Phys. Rev. B 77 (2008) 073306.
- [10] M. Bolduc, C. Awo-Affouda, A. Stollenwerk, M.B. Huang, F.G. Ramos, G. Agnello, V.P. LaBella, Phys. Rev. B 71 (2005) 033302.
- [11] M. Bolduc, C. Awo-Affouda, F. Ramos, V.P. LaBella, J. Vac. Sci. Technol. A 24 (2006) 1648.
- [12] C. Awo-Affouda, M. Bolduc, M.B. Huang, F. Ramos, K.A. Dunn, B. Thiel, G. Agnello, V.P. LaBella, J. Vac. Sci. Technol. A 24 (2006) 1644.
- [13] S.Q. Zhou, K. Potzger, G.F. Zhang, A. Mücklich, F. Eichhorn, N. Schell, R. Grötzschel, B. Schmidt, W. Skorupa, M. Helm, J. Fassbender, Phys. Rev. B 75 (2007) 085203.
- [14] F.M. Zhang, X.C. Liu, J. Gao, X.S. Wu, Y.W. Du, H. Zhu, J.Q. Xiao, P. Chen, Appl. Phys. Lett. 85 (2004) 786.
- [15] Z.Z. Zhang, B. Partoens, K. Chang, F.M. Peeters, Phys. Rev. B 77 (2008) 155201.
- [16] L.J. Gao, L. Chow, R. Vanfleet, K. Jin, Z.H. Zhang, X.F. Duan, B. Xu, B.Y. Zhu, L.X. Cao, X.G. Qiu, B.R. Zhao, Solid State Commun. 148 (2008) 122.
- [17] J.H. Yao, H.H. Lin, T.S. Chin, Appl. Phys. Lett. 92 (2008) 242501.
- [18] Y.L. Soo, J.H. Yao, C.S. Wang, S.L. Chang, C.A. Hsieh, J.F. Lee, T.S. Chin, Phys. Rev. B 81 (2010) 104104.
- [19] Y.H. Kwon, T.W. Kang, H.Y. Cho, T.W. Kim, Solid State Commun. 136 (2005) 257.
- [20] Y.H. Kwon, T.W. Kang, Y. Shon, H.Y. Cho, H.C. Jeon, Y.S. Park, D.U. Lee, T.W. Kim, D.J. Fu, X.J. Fan, Solid State Commun. 147 (2008) 161.
- [21] Z. Iqbal, S. Veprek, J. Phys. C 15 (1982) 377.
- [22] W. Henrion, H. Lange, E. Jahne, M. Gehler, Appl. Surf. Sci. 70 (1993) 569.
- [23] A. Borghesi, A. Piaggi, A. Franchin, G. Guizzetti, F. Nava, G. Santoro, Europhys. Lett. 11 (1990) 61.
- [24] H. Lange, M. Gehler, W. Henrion, F. Fenske, I. Sieber, G. Oertel, Phys. Stat. Sol. B 171 (1992) 63.
- [25] V. Bellani, G. Guizzetti, F. Marebelli, A. Piaggi, A. Borghesi, F. Nava, V.N. Antonov, V.I.N. Antonov, O. Jesen, O.K. Andersen, V.V. Nemoshkaleiko, Phys. Rev. B 46 (1992) 9380.
- [26] J.S. Lu, H.B. Yang, B.B. Liu, J. Han, G.T. Zou, Mater. Chem. Phys. 59 (1999) 101.
- [27] H.C. Barshilia, K.S. Rajam, Appl. Surf. Sci. 255 (2008) 2925.
- [28] M. Bolduc, C. Awoaffouda, A. Stollenwerk, M. Huang, F. Ramos, V. LaBella, Nucl. Instrum. Methods B 242 (2006) 367.
- [29] W.P. Osmond, Proc. Phys. Soc. 79 (1962) 394.
- [30] I.J. Ohsugi, T. Kojima, I.A. Nishida, Phys. Rev. B 42 (1990) 10761.
- [31] A. Kaminski, S.D. Sarma, Phys. Rev. Lett. 88 (2002) 247202.